Pergamon

PII: S0042-6989(97)00280-0

Vision Res., Vol. 38, No. 7, pp. 973–983, 1998

Printed in Great Britain
0042-6989/98 $19.00 + 0.00

Dichromatic Color Vision at High Light Levels: Red/Green Discrimination using the Blue-Sensitive Mechanism*

MATTHEW J. MCMAHON,†‡ DONALD I. A. MACLEOD†

Received 4 December 1996; in revised form 2 July 1997; in final form 4 August 1997

Three red/green blind observers (dichromats) performed a wavelength discrimination task over a wide range of intensity levels. As expected, discrimination failed in the entire red/green spectral range at the low intensities typically used in wavelength discrimination experiments, but at very high intensities (at or above 10 000 td) discrimination was well maintained into the red/green range. The following experiments demonstrate that dichromats are able to utilize signals from the blue-sensitive cones (S-cones) to mediate color discrimination throughout the spectrum at high intensities, and they provide an estimate of S-cone sensitivity throughout the visible spectrum.

Color Wavelength discrimination Dichromacy S-cones

INTRODUCTION

In the latter part of the 19th century, Hermann von Helmholtz devised a theory of wavelength discrimination based on differential quantum catches of three different photoreceptor types, each with a different characteristic spectral sensitivity (Helmholtz, 1896). The basic assumption of Helmholtz's theory is that color discrimination is based on a comparison of the excitations produced by a stimulus in the three underlying processes, or photoreceptor types, and the precision of each comparison is given by Weber's Law, which states that a just detectable change in excitation requires a constant proportion of the initial stimulus value. In order to apply this model, we must first know which of these processes are stimulated at each wavelength and intensity. S-cone sensitivity viewed on a linear scale drops to nearly zero at approximately 550 nm. Above this wavelength, normal trichromats are able to compare signals from the medium wavelength sensitive cones (M-cones) and long wavelength sensitive cones (L-cones) to maintain discrimination. However, red/green blind dichromats derive useful signals from only one cone type in the red/green spectral range and hence show little or no wavelength discrimination. If, however, we can assume that the photoreceptors follow Weber's Law, then it is the *log* of S-cone sensitivity which is important. This is because a just noticeable difference in wavelength will then require a constant *percentage* difference in photoreceptor stimulation, or a constant change in the log sensitivity. If S-cone sensitivity is plotted as a function of wavelength, it is evident that the S-cones have a steep gradient of log sensitivity throughout almost the entire visible spectrum (see Fig. 1). However, the utilization of the S-cones across the spectrum requires that they be stimulated

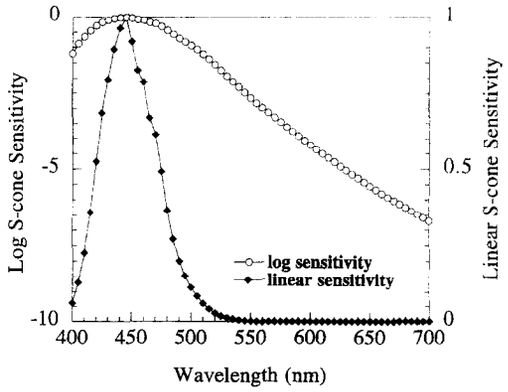

FIGURE 1. S-cone spectral sensitivity from Stockman *et al.* (1993). Although the linear sensitivity drops to nearly zero at 540 nm, the log sensitivity maintains a steep slope throughout most of the visible spectrum. With sufficiently intense red/green stimuli, S-cones should be able to provide sufficient signals to mediate wavelength discrimination across the visible spectrum.

*A previous version of this work was presented at the 1994 ARVO annual meeting (McMahon & MacLeod, 1994).

†University of California San Diego, Department of Psychology, La Jolla, CA 92093, U.S.A.

‡To whom all correspondence should be addressed [*Email*: mm@ucsd.edu].

above their functional threshold*. This requirement is not fulfilled in the red/green spectral range at the dim intensities customarily used for monochromatic stimuli, but it may be if the red/green stimuli are sufficiently intense.

How can wavelength discrimination be predicted based only on the assumption of Weber's Law at the receptoral level? Consider the case of a protanope. Discrimination in these individuals is achieved by a comparison of S-cone and M-cone signals generated by a stimulus. But because Weber's Law applies, it is the *logs* of the cone excitations that are relevant. Color discriminability is judged after a suitable adjustment of the relative intensity of the two lights to be discriminated. Since in a bipartite field, such as we use in our color discrimination measurements, a minimally distinct border occurs when fields are equated for the long wavelength cones, regardless of the difference for the S-cones (Tansley & Boynton, 1978), we assume that the intensity adjustment is used to equate the excitations of the M-cones of the protanope. This is done by setting the intensities E1 and E2 in the ratio of the M-cone sensitivities, M2/M1, so that Log(E1) − Log(E2) = Log(M2) − Log(M1). Once this has been done, the S-cone excitations for the two stimuli compared will differ. The logarithmic difference is: Log(S1) + Log(E1) − Log(S2) + Log(E2), or (Log(S1) − Log(M1)) − (Log(S2) − Log(M2)). The derivative of this with respect to wavelength is proportional to the percent difference in S-cone excitation for M-cone equated lights that differ by one (small) unit in wavelength. The *reciprocal* of the derivative is proportional to the wavelength difference needed for a criterion small percentage difference in S-cone excitation. This scheme (shown in Fig. 2) predicts good wavelength discrimination throughout the visible spectrum at all intensities, without the failure in the red/green range that is normally characteristic of protanopes. That failure is presumably due to the failure of red or green lights to reach the functional threshold of the S-cones. In such a case, Weber's Law will not apply. In order to accommodate this, our model of receptoral differential sensitivity includes (following Helmholtz) an absolute threshold intensity range as well as a Weber intensity region and a saturation or overloading intensity region, as can be seen in Fig. 3(a). In the model, Δ^*I is the threshold for a change in intensity for a given photoreceptor, w is the Weber Fraction, I_o is the threshold intensity, and c is the saturation constant.

Our assumption that an observer always makes a precise match for M-cones and then uses the S-cone difference to evaluate the color difference is not only simple and consistent with the minimally distinct border observations of Tansley and Boynton (1978), it is also plausible, at least as an approximation, on the grounds that M-cones have a much greater differential sensitivity than S-cones [Weber fraction approximately 5-times lower by Stiles's estimates (Stiles, 1959)]. Consequently,

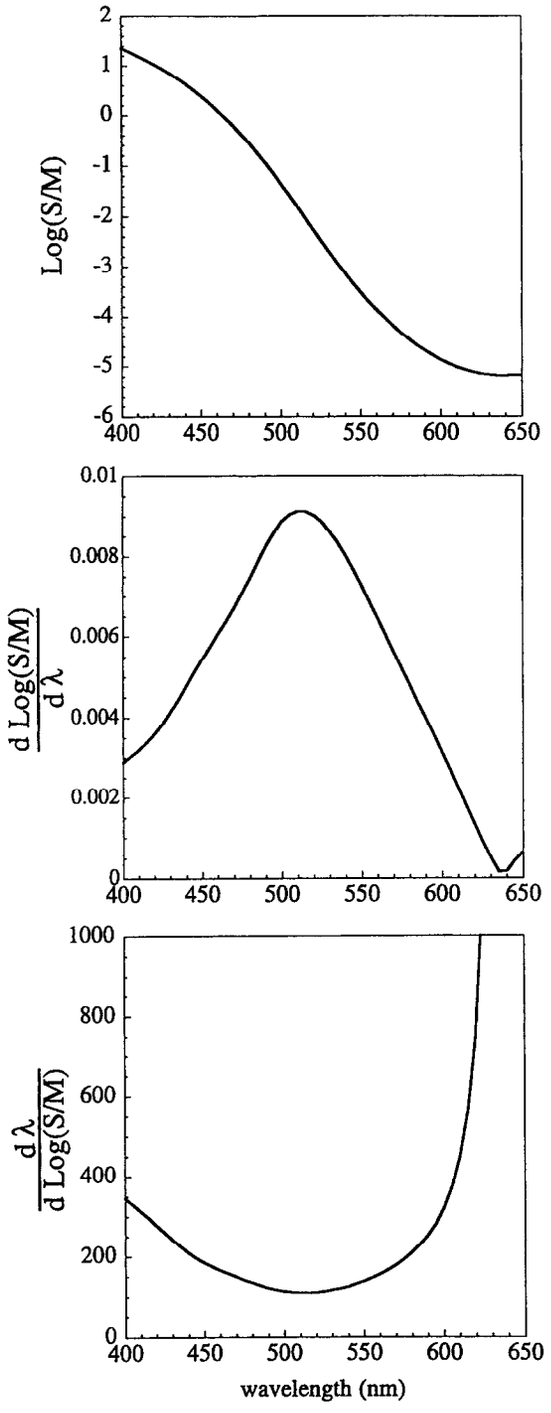

FIGURE 2. Weber's Law at the receptoral level can be used to predict wavelength discrimination for a protanopic observer. A color difference can be recognized only through a difference in the ratio of the S-cone and M-cone excitations for two wavelengths. But because Weber's Law applies, it is the log of the ratio of the sensitivities which is of interest. We differentiate this with respect to wavelength in order to determine the gradient, or slope, of the function. This is proportional to the percent difference in S-cone excitation for M-cone equated lights that differ by one (small) unit in wavelength. Finally, we consider the reciprocal of that gradient, because good wavelength discrimination is expected where the log of the cone sensitivity ratio has the highest slope.

*Electrophysiological experiments (Baylor & Hodgkin, 1974) have shown that the threshold response of cones is linear, with no threshold nonlinearity. "Subthreshold" signals are merely lost in the noise at the cone level and thus fail to reliably activate more central neurons (Donner, 1992).

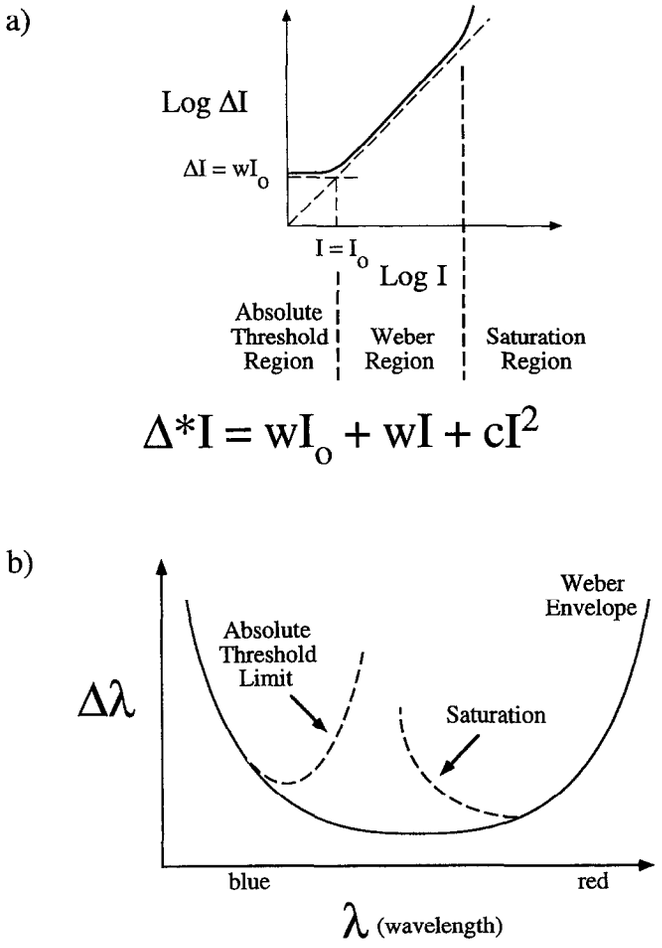

FIGURE 3. (a) Modified version of Weber's Law used to model wavelength discrimination: Δ^*I is the threshold for a change in intensity for a photoreceptor, w is the Weber Fraction, I_0 is the threshold intensity, and c is the saturation constant. This model produces three distinct intensity ranges: one dominated by the absolute threshold term, a Weber region, and a region in which the saturation term causes an upward deviation from Weber's Law. (b) The Weber Envelope (solid line) would be predicted at any intensity by a model of wavelength discrimination based on pure Weber's Law behavior at the receptoral level (e.g. that of Fig. 2). The predictions of the modified Weber's Law used in our model are shown with the dashed lines. The inclusion of an S-cone absolute threshold produces deviations at long wavelengths and low intensities. In this case, protanopes only have access to signals from the M-cones and discrimination fails. The inclusion of an S-cone saturation term would predict a failure in discrimination at short wavelengths and high intensities.

the intensity setting for minimal discriminability will be very close to M-cone equality (see Appendix A). We calculate the threshold color difference by implementing the receptoral model for S-cone responses only, as if the stimuli compared are always equated for the M-cones, rather than being set (as Helmholtz assumed) at a compromise between S- and M-cone equality. As Appendix A shows, any inaccuracy resulting from this assumption is very slight.

Weber's Law if applied exactly, with no saturation or threshold effects, would predict that wavelength discrimination should follow a smooth envelope throughout the visible spectrum and be completely independent of the intensity level at which the discriminations are assessed. But in reality, Weber's Law fails and at low and moderate intensities we expect to see the effect of absolute threshold. As wavelength is increased into the red/green range, S-cones can no longer produce reliable signals and as a result wavelength discrimination deteriorates. This is seen in classical wavelength discrimination curves measured at low and moderate intensities, which show a complete failure of discrimination above 520 nm (the so-called Rayleigh region) that is the defining characteristic of red/green dichromacy. It has been shown that protanomalous observers (Thomson & Trezona, 1951) and deuteranopes (Walraven & Bouman, 1966) display their best wavelength discrimination at an optimum wavelength that is luminance dependent, being longer at higher luminance. Although this change was modeled by Walraven and Bouman by an arbitrary adjustment of a parameter in their color model, some such change is expected simply on the basis of the existence of an S-cone absolute threshold (Mollon, Estévez & Cavonius, 1990). Our first experiment extends this observation by the use of much higher luminances and the results are fit using a simple model invoking Weber's Law together with an absolute threshold. At high intensities, we also allow for a possible overloading or saturation of the S-cone system at short wavelengths. Early evidence for this comes from what has been called the König–Dieterici anomaly (König & Dieterici, 1884). A decrease in intensity at 460 nm was shown to yield better discrimination ability, presumably by releasing the S-cones from overload or saturation. Mollon and Polden have also described saturating behavior of the S-cone signal (Mollon & Polden, 1977). This saturation may take place at a post-receptoral opponent processing site (Pugh & Larimer, 1980); (Polden & Mollon, 1980); (Mollon & Estévez, 1988). The wavelength discrimination envelope predicted from Weber's Law alone and the modifications produced by the inclusion of a saturation and a threshold term are schematized in Fig. 3(b).

The preceding analysis implies a surprising consequence: high light levels should allow red/green dichromats to utilize S-cone signals to support good wavelength discrimination across the visible spectrum. In the following experiments this prediction is tested and confirmed.

METHODS

Stimuli were presented by means of a computer controlled three-channel Maxwellian view system. A 12 Volt, 100 Watt tungsten halogen lamp served as the light source for all three channels. Two channels provided monochromatic light for left and right halves of a 3 deg circular field. Each of these channels contained a variable-wavelength interference filter (rainbow wedge) manufactured by JENA^{ER} Glaswerk Schott and Gen., Mainz and a 0–4 log unit graded neutral density filter which were driven by stepping motors with a resolution of 0.3 nm in wavelength and 0.007 log units in density. The Maxwellian image was focused onto the rainbow wedge and provided a pseudo-monochromatic beam. The

spectral power density profiles were approximately gaussian, with a bandwidth (full width at half height) of roughly 15 nm at all wavelengths. Additional fixed value neutral density filters (Oriel reflection type) were added when necessary. The optical paths of the first two channels were completely separated to minimize unnecessary reductions in light intensity. The boundary between the two half-fields was produced by the sharp edge of a thin front silvered mirror, with one beam being transmitted past the edge of the mirror and the other beam being reflected by it. A Wratten #8 filter was used in the common path for wavelengths greater than 470 nm in order to block any weak shorter wavelength light passed by the variable-wavelength wedges. The third channel contained 420 nm light of fixed intensity (Oriel interference filter and Wratten neutral density filters) and was superimposed on one of the previously described channels in order to produce the stimuli for dichromatic matching.

Radiances of the stimuli passed by the variable-wavelength filters were measured with a UDT Model 370 Optometer. The wavelength scale was calibrated using the UDT Optometer and narrowband interference filters and was verified using a helium–neon laser. The spectral transmission of the variable neutral density wedges was measured at their half-maximum density positions (in 20 nm steps). A wavelength-dependent density-scaling factor was used to correct for non-neutrality at all wedge positions. Interpolated values of absolute wavelength and neutral density for each motor step were stored in calibration look-up tables. Conversions to photometric quantities were performed using the Judd-modified $V(\lambda)$ (Wyszecki & Stiles, 1982). These calibrations of the variable-wavelength and variable neutral density filters were done *in situ*. All other neutral density and blocking filters used in the experiment were also calibrated *in situ*.

Additional calibration was conducted in order to quantify the amount of short wavelength light which leaked through the variable-wavelength wedges and produced a skirt of shorter wavelength light. A Photo Research PR704 spectroradiometer was used to measure the spectral output of the wavelength wedges at the 620 and 650 nm positions with no blocking filters. Because this device samples the entire spectral range simultaneously, its integration time is determined by the energy at the peak wavelength. This made it very difficult to measure the off-peak regions of a narrowband stimulus. With the short integration times used for the 620 and 650 nm stimuli, the detector noise was 5×10^{-4} times the peak spectral power density and this noise level was not exceeded for wavelengths below 560 nm. Additional *in situ* scans were therefore taken with the addition of a Newport short wavelength pass filter (10SWF-600), which severely attenuated the energy at the peak wavelength. This allowed the PR704 to obtain more accurate measurements of the short and middle wavelength regions by using very long integration times (in the order of 30 sec, as opposed to around 100 msec without the filter). We then corrected these scans for the transmission of the short wavelength pass filter. This method allowed us to obtain spectral scans which covered an intensity range of greater than 5 log units, dropping to the level of the detector noise (2×10^{-5} times peak for the 620 nm stimulus and 1×10^{-6} times peak for the 650 nm stimulus) at 540 nm. The 620 nm stimulus was then revealed to have a slight shoulder in its spectral power distribution at 560 nm, where the spectral power density was 2.75×10^{-4} times the peak. The 650 nm stimulus had slight shoulders of 10^{-3} times peak at 610 nm and 5×10^{-5} times peak at 560 nm.

To achieve valid measurements of the spectral output below 540 nm, the wavelength wedge was removed from the system. A Bausch and Lomb monochromator was used to shine high intensity 420, 460, 480, 500, 520, and 540 nm light through the wedge at its 620 and 650 nm positions. Informal checks were made at other wavelengths to justify interpolation. The transmission of the wavelength wedge in this spectral range was calculated by taking the ratio of the wavelength wedge attenuated monochromator output intensity to the unattenuated monochromator output. To calculate the spectral output of the wavelength wedge at the sampled wavelengths, the transmission values were multiplied by the spectral output of system measured without the wavelength wedge in place. The resulting values at 540 nm were well matched to the values measured *in situ* with the direct spectroradiometric technique described above. For the 620 nm stimulus, the spectral outputs for 420, 460 and 480 nm were all less than 10^{-10} times the peak spectral power density. The output at 500 nm was 4×10^{-10} relative to peak and the output at 520 nm was 2×10^{-8} relative to peak. For the 650 nm stimulus, the spectral output values calculated for all wavelengths below 540 nm were less than 10^{-10} relative to the peak. Whether due to detector noise or not, these insignificantly small spectral power densities measured from 400–540 nm were adopted along with the *in situ* PR704 measurements from 540 to 700 nm. In this way we were able to obtain spectral output functions which covered a 10 log unit range. Wavelength dependent corrections based on these spectral output measurements are described in subsequent sections.

When necessary, we employed two rod bleaching procedures. A 3 deg rod bleach was generated with a 500 nm stimulus at maximum intensity for 66 sec. This produced 7 log td sec of integrated retinal illuminance. Alternatively, a 9 deg bleach could be generated by removing a circular field stop from the apparatus. Wavelength discriminations were made 5–10 min after the bleach, after which time the rod bleach was repeated.

The observers were all males with protanopic color vision. MM and ML's protanopia have been tested extensively, and have been verified in numerous laboratories. Observer ST was characterized as a protanope on the basis of tests with a Nagel anomaloscope (in which he readily matched every red/green ratio to yellow with an intensity adjustment only) and

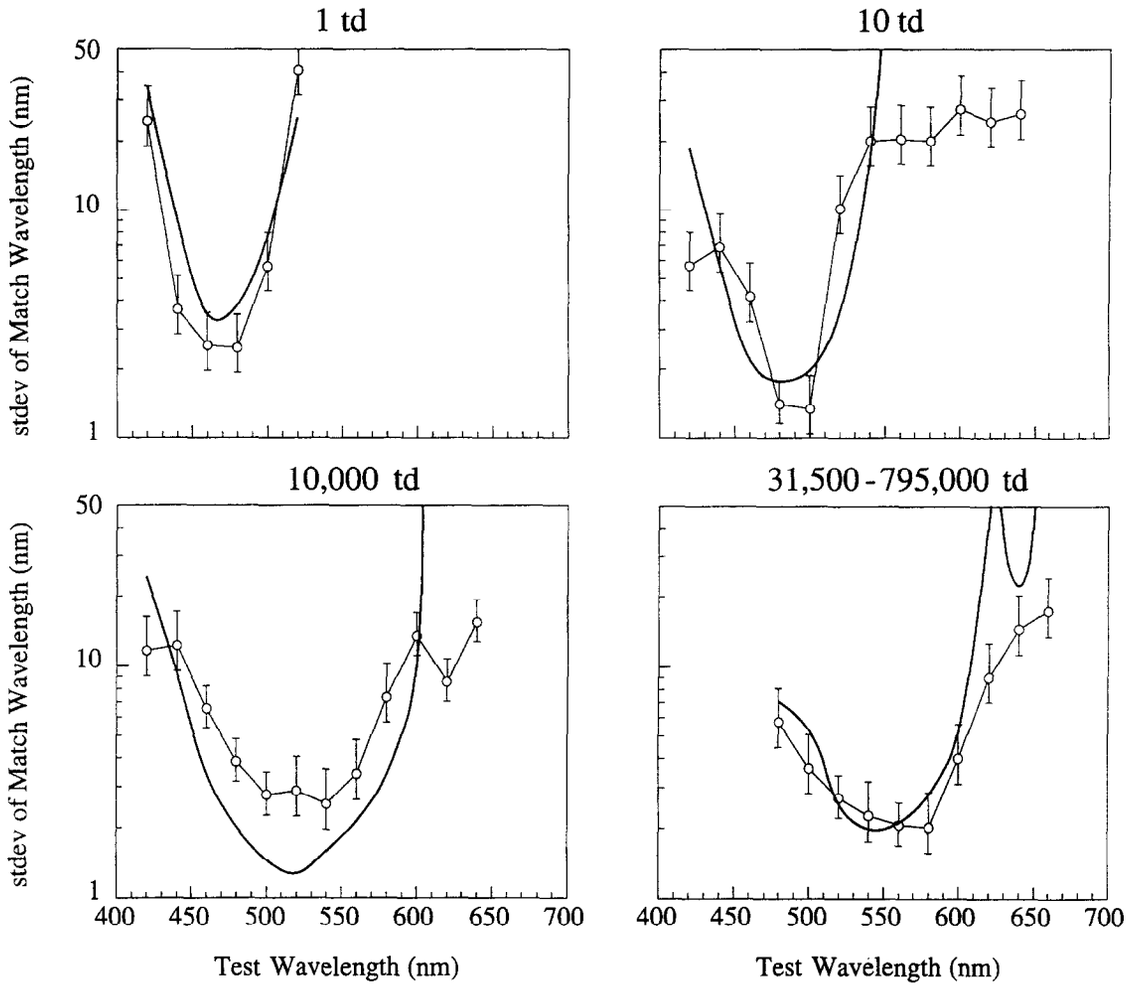

FIGURE 4. Wavelength discrimination curves for observer MM measured at different intensity levels are plotted, together with predictions of the Weber's Law receptoral model of wavelength discrimination (bold lines). At short wavelengths, increasing the intensity produces a decrease in discrimination ability. At long wavelengths, increasing intensity led to an increase in discrimination performance by providing enough intensity to allow S-cones to contribute to the discriminations. At the highest intensity level, very good discrimination was maintained in the red/green range to about 600 nm, where dichromats traditionally have no discrimination ability.

performance on the Ishihara Pseudoisochromatic Plate test.

Experiment 1: wavelength discrimination

Procedure. The first experiment consisted of the measurement of wavelength discrimination curves at four different intensity levels. The observer fixated the center of the bipartite field. On each trial, one side of the bipartite field (the "standard") was set in wavelength and intensity by the computer and the other side (the "match") could be continuously varied in both dimensions by the observer using a computer track ball. Vertical movements varied the intensity of the match field, horizontal movements varied the wavelength of the match field, and a button press signaled the computer to record a setting. After each setting was recorded, the match field was repositioned randomly in wavelength and intensity and the standard field was set for the next trial to an intensity and wavelength randomly selected from the set of conditions being examined.

A session consisted of wavelength discrimination measurements at a fixed intensity and at a number of wavelengths. The polarity of the half-fields (left half-field = standard or match) was randomly chosen for each presentation. The measure of performance was the standard deviation of a minimum of 24 wavelength settings. This "method of average error" procedure produces a difference limen which is more objective than one derived from settings in which the match field is positioned to be in the subject's opinion "just noticeably different" from the standard field.

Results. Wavelength discrimination curves were measured for observer MM at 1, 10, 10 000 td and at the maximum output of the system. This maximum output varied with wavelength from 31 500 to 795 000 td because of the non-uniform spectral output of the source. The discrimination curves are plotted together in Fig. 4. The discrimination envelope shifts from a minimum at 490 nm (blue–green) for the 1 td condition to approximately 560 nm (yellow) at the maximum output condition. At short wavelengths, such as 450 nm, increasing intensity leads to a decrease in performance. At longer

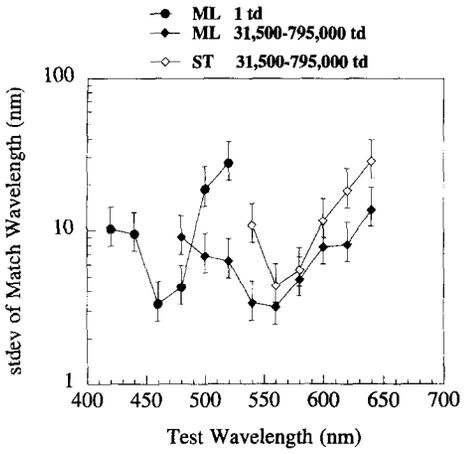

FIGURE 5. Wavelength discrimination curves for observers ML and ST. Results are similar to those of observer MM. In the high intensity condition, discrimination was maintained in the red/green range.

wavelengths, such as 550 nm, the increase in stimulus intensity leads to an improvement in wavelength discrimination performance.

These observations were replicated with naïve observers ML and ST (Fig. 5). ML's discrimination envelope shifts from a minimum at 460 nm for the 1 td condition to 560 nm for the maximum intensity condition. In the maximum intensity condition, ML and ST's peak discrimination ability occurred at 560 nm (yellow), with useful discrimination extending into the red. Previous research has shown that there are only minor quantitative individual differences in the wavelength discrimination performance of dichromatic observers (Wright, 1946).

Because the standard deviation of a normally distributed population follows a χ^2 distribution, 95% confidence intervals were constructed around the data points using the expression below (Hays, 1988):

$$stdev\sqrt{\frac{(N-1)}{\chi^2_{(N-1;0.025)}}} \text{ to } stdev\sqrt{\frac{(N-1)}{\chi^2_{(N-1;0.975)}}}$$

The Weber's Law receptoral model of wavelength discrimination was used to predict discrimination functions at the intensity levels used in our experiment (bold line, Fig. 4). The resulting equation and parameter values for the model are given below:

$$\Delta^* I = w(I + I_o) + cI^2$$

$$w = 0.0558$$

$$I_o = 0.547 \text{ td at } 440 \text{ nm}$$

$$c = 4.62 \times 10^{-6} \text{ td at } 440 \text{ nm}$$

The semi-saturation intensity, the intensity at which the threshold would be twice that given by Weber's Law alone, is equal to w/c (1.21×10^4 td at 440 nm).

All of the qualitative features of the wavelength discrimination data are captured by the model, although there are small luminance-dependent differences in absolute performance level.

In order determine if the flattening of the wavelength discrimination functions at long wavelengths for the 10 td intensity was a result of rod participation, MM repeated the 580 and 640 nm 10 td measurements after a 3 deg rod bleach (see Methods). The standard deviations of the 24 matches per wavelength underwent a statistically significant increase to 38.8 and 39.6 nm (from 20.1 and 26.4 nm without rod bleaching, respectively) suggesting that the residual long wavelength discrimination in the 10 td condition was partially rod mediated. The high but still finite standard deviations recorded in the rod bleached condition may not imply true discrimination at long wavelengths at all, but could be an artifact of the limited wavelength range which the observer has available to make settings. If the observer sets the match wavelength randomly between 550 nm and the longest wavelength which he can achieve enough intensity to match the stimulus (determined by the filter configuration for the session) for all stimuli within that range, we would expect the standard deviation of his settings to be equal to range/$(2\sqrt{3})$. This standard deviation would be 40.4 nm for 580 nm stimuli and 46.2 nm for 640 nm stimuli and is well within the confidence intervals for the measured rod bleached discriminations.

To assess whether MM had no discrimination ability in this range, one side of the field was set to 10 td 650 nm and the match field was set to a random luminance 560 nm. After a 3 deg rod bleach, the observer was instructed to vary only the luminance of the match field and to decide if an acceptable match was possible. MM was able to make acceptable matches, confirming that the residual long wavelength discrimination in the 10 td condition resulted from some combination of rod participation and limited wavelength range.

To ensure that the good long wavelength discrimination at maximum intensity was not due to rod participation (perhaps due to a scattered light penumbra) the 600 nm maximum intensity point was remeasured after a 9 deg rod bleach (see Methods). The resulting standard deviation was 2.6 nm, which was not significantly different from the previously measured value.

Experiment 2: dichromatic matching

Procedure. The second experiment was a dichromatic matching task, with the right half-field consisting of a combination of a fixed intensity of the blue primary (420 nm) and various intensities of the red primary (620 nm) and the left half-field being under control of the observer. The red primary channel contained a Wratten #8 filter to block any short wavelength light which may have been passed by the variable-wavelength wedge. The match channel also contained a Wratten #8 filter for the high red/blue primary ratio conditions. For each red/blue ratio, the observer set a monochromatic wavelength and intensity which matched the test field exactly. In order to push the sensitivity estimates to longer wavelengths, a condition was included which contained no blue primary

and the maximum intensity of a 650 nm red primary in the "standard" channel.

The presentation of red/blue ratios was random. After each setting was recorded, the match field was set randomly in wavelength and intensity.

The specified match wavelengths were adjusted to take into account the finite bandwidth of the variable-wavelength filters. In this procedure, the Stockman, MacLeod and Johnson (1993) cone sensitivities were used to determine which strictly monochromatic wavelength had the same protanopic color (same ratio of S-to M-cone excitation) as the gaussian spectral energy profile passed by the variable-wavelength filter. This correction was typically only 1 or 2 nm. The corrected wavelengths, λ_{corr}, are the ones used in plotting the data.

An additional correction was calculated to allow for the short wavelength skirt (not well described by a gaussian) which was transmitted by the wavelength wedges. The spectral output functions, $E(\lambda)$, for the nominal 620 and 650 nm stimuli were multiplied by the S-cone spectral sensitivity function, $S(\lambda)$ (Stockman *et al.*, 1993), to produce a measure of S-cone excitation. The theoretical S-cone sensitivity for these stimuli were then calculated with the following formula:

$$S_F = \frac{\int E(\lambda)S(\lambda)d\lambda}{\int E(\lambda)d(\lambda)}.$$

A filter-dependent sensitivity correction factor (quantifying the inexactness of our gaussian approximation for the spectral power density) was then computed relative to the sensitivity at the bandwidth-corrected wedge wavelength (λ_{corr}): $\log(S_F/S(\lambda_{corr}))$. For 620 nm this correction was 0.004 and at 650 nm 0.077. These calculations do not take into account the Wratten #8 blocking filter that was present during the experiment. If the calculations are repeated taking into account the density of the Wratten #8 filter, the correction becomes −0.056 for 620 nm and 0.028 for 650 nm. If the corrections are calculated using the Lamb (1995) S-cone spectral sensitivity, they are still less than 0.1 at 620 and 650 nm.

An unbiased representation of the spectral sensitivity from the dichromatic matching experiment results if points are plotted against λ_{corr} and adjusted vertically (log sensitivity) by $-\log(S_F/S(\lambda_{corr}))$ for each wavelength. Points were plotted against λ_{corr}, as mentioned above, but the vertical corrections described above were not made because they were considered insignificantly small.

MM's macular pigment density was measured by performing an M-cone-based bipartite field brightness match between a fixed intensity 588 nm and an adjustable 460 nm in the presence of an intense 420 nm background. The polarity of the half-fields was varied between settings to control for retinal inhomogeneity. This measurement was made foveally and at 10 deg eccentricity. The difference in the 460 nm log intensity values for the foveal and 10 deg conditions is the macular pigment density at 460 nm. To avoid any error caused by optical density differences between the fovea and periphery, we chose two wavelengths which equally excite the M-cones. As a result, the broadening of the M-cone spectral sensitivity by self-screening in the fovea will equally affect both sides of the bipartite field, and the ratio will be unaffected. This method produced a peak macular pigment density of 0.712.

Results. By suitably adjusting wavelength and intensity, MM could always find some spectral light to match exactly each red/blue mixture, and these matches were unique (aside from random error). He therefore satisfies a strict criterion of dichromacy under the conditions of the experiment, in the sense that two adjustments are necessary and sufficient for an exact match, as if the two lights must be equated in their action on two spectrally selective photoreceptor mechanisms.

For each match recorded by observer MM, we know the radiances of the 620 and 420 nm primary lights presented, and the wavelength and radiance of the spectral light chosen to match that purple mixture. We wish to infer the spectral sensitivities of the participating mechanisms (particularly the shorter wavelength sensitive mechanism), but these are unfortunately not defined uniquely by the data: given some pair of spectral sensitivities exactly consistent with the data, any pair of mechanisms with sensitivities that are a linear combination of the given pair will also fail to distinguish between the matched fields. If the short wavelength mechanism were completely insensitive to the 620 nm primary, its spectral sensitivity could be estimated from the radiance of each spectral test light required for a match to the fixed intensity short wavelength primary, while variation in the intensity of the long wavelength primary causes the chosen test wavelength to traverse the spectrum. In all such matches the short wavelength mechanism receives the same stimulation, due entirely to the fixed short wavelength primary on one side of the field or to the chosen wavelength and radiance of the matching monochromatic light on the other side of the field. The spectral sensitivity estimated on this basis peaks in the violet, with a smooth descent of log sensitivity up to 600 nm, but log sensitivity then falls precipitously at longer wavelengths, becoming infinitely negative at 620 nm. Other possible spectral sensitivities are obtained by assuming non-zero sensitivity of the short wavelength mechanism to the 620 nm primary. These spectral sensitivities are linear combinations of the radiances of the 420 and 620 nm primaries in the presented mixture (corresponding to the stimulation of the short wavelength mechanism by the mixture) divided by the radiance of the spectral light chosen to match it. Only one such choice (subject to a tolerance of roughly a factor of two in relative sensitivity to 620 and 420 nm) yields a smoothly descending log sensitivity without an obvious upward or downward inflection in the orange. This choice assigns the short wavelength mechanism a sensitivity at 620 nm which is very small relative to 420 nm, and generates the spectral sensitivity shown in Fig. 6.

MM's measured peak macular pigment density (0.712) is much higher than the average value (0.347) reported by Stockman *et al.* (1993). In order to avoid an unrepre-

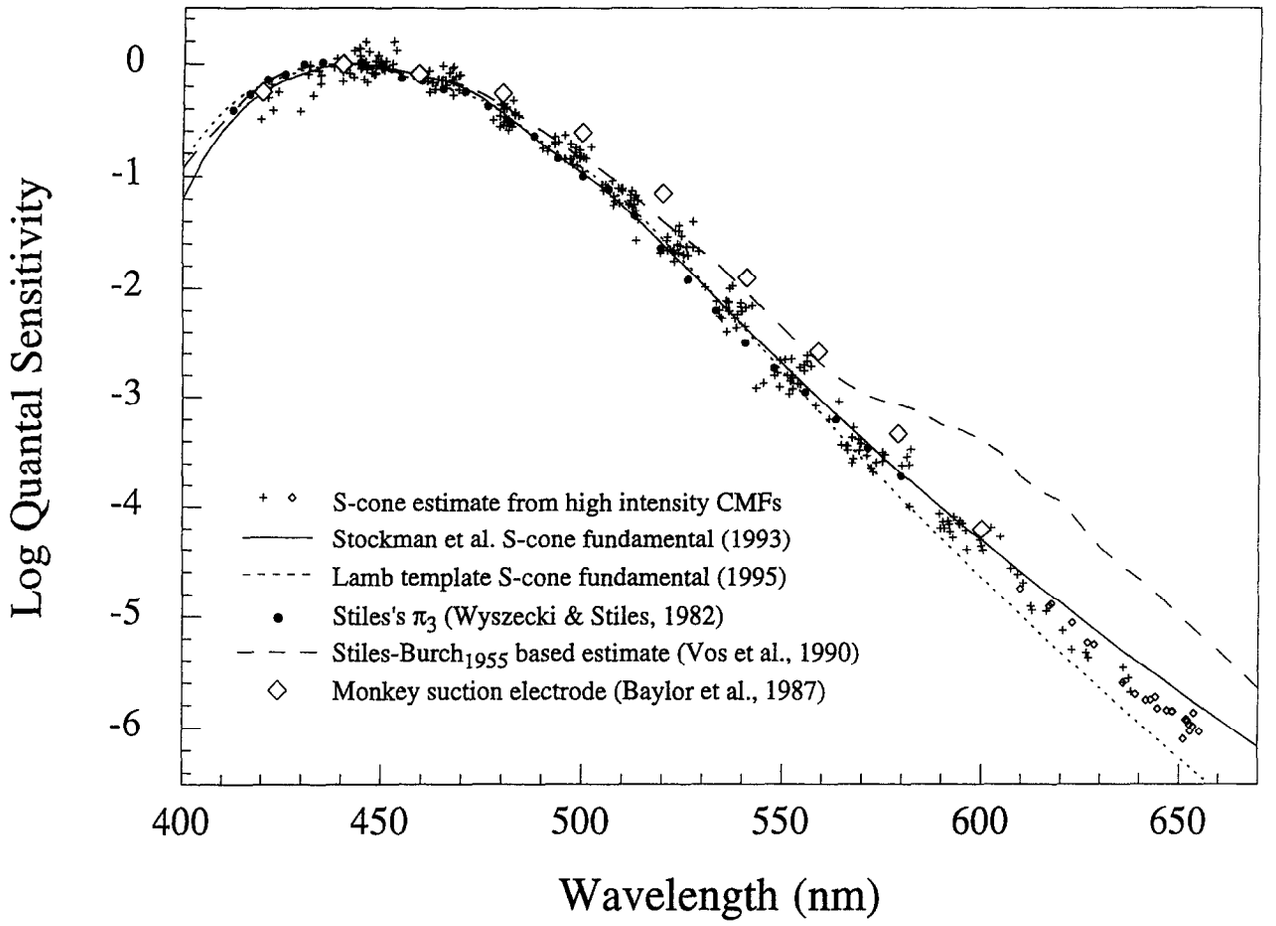

FIGURE 6. Spectral sensitivity of the mechanism derived from MM's high intensity dichromatic matching data plotted together with other S-cone sensitivity estimates. These data confirm that the high intensity discriminations in Experiment 1 are S-cone-mediated. Small diamonds represent data from the maximum red primary plus no blue primary condition (see text). The data points have been adjusted to a peak macular pigment density of 0.347 (from MM's measured density of 0.712) for ease of comparison. Stiles's π_3 field sensitivity (filled circles) from Table 2 (7.4.3) of Wyszecki and Stiles (1982). S-cone fundamentals: Stiles-Burch (1955) based estimate (Vos *et al.*, 1990) (dashed line), Stockman *et al.* (1993) (solid line) and Lamb (1995) [calculated with λ_{max} = 421 nm, 0.347 peak macular pigment density, 0.4 photopigment density and the Stockman *et al.* (1993) adjusted lens density] (dotted line). Physiological data: suction electrode recordings (Baylor *et al.*, 1987) (large diamonds) corrected for macular pigment, lens, and axial photopigment density (same values as used for Lamb above). Unlike other available color matching data, our S-cone sensitivity estimate is very similar to suction electrode recording measurements and also to Stiles's π_3 field sensitivity measurements.

sentatively low sensitivity estimate at short wavelengths, the data points have been adjusted to a peak macular pigment density of 0.347 by adding a 0.365 peak density macular pigment template (Wyszecki & Stiles, 1982) to the data. The data were then normalized to the mean of the group of data points centered at 445 nm. The grouping of data points reflects multiple matches made to each red/blue primary ratio.

DISCUSSION

Model for wavelength discrimination

The results of the wavelength discrimination measurements confirm the prediction that increased light levels allow "red/green blind" protanopes to achieve good wavelength discrimination, even in the red/green spectral range. The data are in approximate agreement with our wavelength discrimination model, which is based on Weber's Law behavior at the photoreceptor level. The traversal of the wavelength discrimination curve to longer wavelengths as intensity is increased is mainly due to the absolute threshold effect included in our model, with the effect of saturation being much smaller.

At long wavelengths, increasing intensity led to an increase in discrimination performance. This behavior is predicted by the model because as S-cones receive enough light to exceed their functional threshold, they can begin to contribute to discrimination. At the highest intensity level, good discrimination was maintained out to 600 nm. In this range, where dichromats traditionally have no discrimination ability at all, their absolute performance levels at the highest intensities are similar to those of normal trichromatic observers.

At short wavelengths, increasing the intensity produced a decrease in discrimination ability in the short wavelength range. This is predicted in our model by the saturation term. The results of our experiments do not allow us to localize the site of saturation. Our model

locates the saturation in the S-cone signal itself for simplicity, whereas in reality other stages of processing may contribute, fed either synergistically (Helmholtz, 1896) or in chromatic-opponent fashion by multiple cone types. Pugh and Mollon (Pugh & Mollon, 1979) have proposed a two-site theory of S-cone processing which predicts many of the results of increment threshold experiments. In this theory, signals originating at the S-cones are first processed at a site controlled by S-cones alone. The second site gain is controlled by a post-receptoral opponent processing stage. Our model contains no adjustments for post-receptoral opponent non-linearities, yet its predictions capture the general pattern of our data.

It may be thought that the increased discrimination ability could be due to large field trichromacy of the observer (Nagy, 1980), perhaps mediated by rod participation (Smith & Pokorny, 1977), but the intensities at which our measurements were made were high enough to completely overload or saturate the rod system. The high intensity discrimination ability also remained intact after a full rod bleach. Moreover, observer MM was able to make perfectly acceptable dichromatic matches between any purple primary ratio and some spectral light. This argues against the utilization of a third cone photopigment or rods in addition to the S-cones and M-cones, for this would have precluded such dichromatic confusions.

S-cone spectral sensitivity

The results of the dichromatic matching confirm the hypothesis that the high intensity wavelength discriminations are indeed S-cone mediated. The S-cone sensitivity derived from our high intensity color matching is plotted with other estimates of S-cone sensitivity in Fig. 6. The results from our high intensity color matching functions are similar to the Stockman *et al.* (1993) estimate throughout the visible spectrum. The deviations seen at short wavelengths are probably due to individual variations in macular pigment density, which are substantial (Webster & MacLeod, 1988). Our S-cone sensitivity estimate is close to suction electrode recording measurements made by Baylor, Nunn and Schnapf (1987) if they are adjusted for macular pigment, lens absorption, and photopigment density, although a small discrepancy remains, supporting the suggestion (Dartnall, Bowmaker & Mollon, 1983) that monkey S-cone λ_{max} is slightly longer than human S-cone λ_{max}. They are also close to Stiles's π_3 field sensitivity measurements (Wyszecki & Stiles, 1982). The Stockman *et al.* (1993) S-cone estimate is based on the Stiles and Burch (1955) 10 deg CMFs to 520 nm. Beyond that it is an extrapolation, but our data suggest that the extrapolation is at least approximately correct. Derivations of S-cone sensitivity based on other available color matching data, including both those of the still current CIE 1931 standard observer (CIE, 1932; see Estévez, 1979) and the color matching functions measured at the NPL in the 1950s (Stiles, 1955, 1959; Vos, Estévez & Walraven, 1990), yield obviously incorrect estimates. This is probably because the intensities in these experiments were too low to excite the S-cones or to fully saturate the rods at long wavelengths.

Lamb has proposed a template for photoreceptor spectral sensitivities which is based on the fact that the absorption spectra of many mammalian photopigments show a common shape when plotted against normalized frequency (ν/ν_{max}) (Lamb, 1995) or equivalently log frequency or log wavelength. The S-cone fundamental generated from this template, like any such template derived from a log ν spectra through a log wavelength shift, is slightly too steep at long wavelengths to provide a good fit to the spectral sensitivity derived from our dichromatic matching data. A more steeply falling S-cone sensitivity, like that of Lamb (1995) or our own Fig. 6, generates a slightly better fit to our high intensity discrimination data because it extends the difference in gradient that provides the basis for color discrimination to longer wavelengths. As seen in Fig. 6, our data lie in between the S-cone predictions of Stockman *et al.* (1993) and Lamb (1995) at long wavelengths. Although theoretical and experimental uncertainties (particularly the uncertain weight for the long wavelength primary, see Experiment 2: Results) prevent our estimate from being exact, our measurements are only consistent with S-cone sensitivities which lie between these two not very divergent estimates.

It is worth noting that it is mainly the slope of the S-cone fundamentals at long wavelengths which is of interest, since the absolute height is very sensitive to the macular pigment and lens absorption corrections and the subsequent renormalization.

In summary, we have shown that S-cones can sustain wavelength discrimination at long wavelengths in dichromats when given adequate stimulation. This discrimination can be accounted for by a Weber's Law receptoral model with an absolute threshold and a high intensity overload or saturation effect. The high intensity color matching functions obtained provide an estimate of S-cone spectral sensitivity throughout the visible spectrum that agrees with existing data and extends them to longer wavelengths.

REFERENCES

Baylor, D. A., Hodgkin, A. L. & Lamb, T. D. (1974). Reconstruction of the electrical responses of turtle cones to flashes and steps of light. *Journal of Physiology, London, 242*, 759–791.

Baylor, D. A., Nunn, B. J. & Schnapf, J. L. (1987). Spectral sensitivity of cones of the monkey *Macaca fascicularis*. *Journal of Physiology (London), 390*, 145–160.

CIE (1932) *Commission Internationale de l'Eclairage Proceedings, 1931*. Cambridge, U.K.: Cambridge University Press.

Dartnall, H. J. A., Bowmaker, J. K. & Mollon, J. D. (1983). Human visual pigments: microspectrophotometric results from the eyes of seven persons. *Proceedings of the Royal Society of London B, 220*, 115–130.

Donner, K. (1992). Noise and the absolute thresholds of cone and rod vision. *Vision Research, 32*, 853–866.

Estévez, O. (1979). On the fundamental data-base of normal and dichromatic color vision. Ph.D. Dissertation, University of Amsterdam.

Hays, W. L. (1988). *Statistics*, 4th ed. New York: Holt, Reinhart and Winston.

Helmholtz, H. v. (1896). *Handbuch der Physiologischen Optik*, 2nd ed. Hamburg and Leipzig: Voss.

König, A. & Dieterici, C. (1884). Über die Empfindlichkeit des normalen Auges für Wellenlängenunterschiede des Lichtes. *Annalen der Physik und Chemie, 22*, 579–589.

Lamb, T. D. (1995). Photoreceptor spectral sensitivities: common shape in the long-wavelength region. *Vision Research, 35*, 3083–3091.

McMahon, M. J. & MacLeod, D. I. A. (1994). Color blind color vision at high light levels: red/green discrimination using the blue-sensitive cones. *Investigative Ophthalmology and Visual Sciences (Suppl.), 35*, 1474.

Mollon, J. D. & Estévez, O. (1988). Tyndall's paradox of hue discrimination. *Journal of the Optical Society of America A, 5*, 151–159.

Mollon, J. D., Estévez, O. & Cavonius, R. (1990). The two subsystems of color vision and their roles in wavelength discrimination. In C. Blakemore (Ed.), *Vision: coding and efficiency* (pp. 119–131). Cambridge, U.K. Cambridge University Press.

Mollon, J. D. & Polden, P. G. (1977). An anomaly in the response of the eye to light of short wavelengths. *Philosophical Transactions of the Royal Society of London B, 278*, 207–240.

Nagy, A. L. (1980). Large-field substitution Rayleigh matches of dichromats. *Journal of the Optical Society of America, 70*, 778–784.

Polden, P. G. & Mollon, J. D. (1980). Reversed effect of adapting stimuli on visual sensitivity. *Proceedings of the Royal Society of London B, 210*, 235–272.

Pugh, E. N. Jr. & Larimer, J. (1980). Test of the identity of the site of blue/yellow hue cancellation and the site of chromatic antagonism in the π_1 pathway. *Vision Research, 20*, 779–788.

Pugh, E. N. Jr. & Mollon, J. D. (1979). A theory of the π_1 and π_3 color mechanisms of Stiles. *Vision Research, 19*, 293–312.

Smith, V. C. & Pokorny, J. (1977). Large-field trichromacy in protanopes and deuteranopes. *Journal of the Optical Society of America, 67*, 213–220.

Stiles, W. S. & Burch, J. M. (1955). Interim report to the Commission internationale de l'eclairage, Zurich, 1955, on the National Physical Laboratory's investigation of colour-matching. *Optica Acta, 2*, 168–181.

Stiles, W. S. (1959). Color vision: the approach through increment threshold sensitivity. *Proceedings of the National Academy of Sciences USA, 45*, 100–114.

Stockman, A., MacLeod, D. I. A. & Johnson, N. E. (1993). Spectral sensitivities of the human cones. *Journal of the Optical Society of America A, 10*, 2491–2521.

Tansley, B. W. & Boynton, R. M. (1978). Chromatic border perception: the role of red- and green-sensitive cones. *Vision Research, 18*, 683–697.

Thomson, L. C. & Trezona, P. W. (1951). The variation of hue discrimination with changes of luminance level. *Journal of Physiology, London, 114*, 98–106.

Vos, J. J., Estévez, O. & Walraven, P. L. (1990). Improved color fundamentals offer a new view on photometric additivity. *Vision Research, 30*, 937–943.

Walraven, P. L. & Bouman, M. A. (1966). Fluctuation theory of colour discrimination of normal trichromats. *Vision Research, 6*, 567–586.

Webster, M. A. & MacLeod, D. I. A. (1988). Factors underlying individual differences in the color matches of normal observers. *Journal of the Optical Society of America A, 5*, 1722–1735.

Wright, W. D. (1946). *Researches on normal and defective colour vision*. London: Henry Kimpton.

Wyszecki, G. & Stiles, W. S. (1982). *Color science: concepts and methods, quantitative data and formulae*, 2nd ed. New York: John Wiley and Sons.

Acknowledgement—Supported by a NSF Graduate Research Fellowship to M.J.M. and NIH Grant EY01711.

APPENDIX A

Simplification of Helmholtz's color difference equation

Figure 7 illustrates the very close relationship between the wavelength discrimination threshold predicted by Helmholtz's line element and the one predicted on our simplifying assumption that the match and reference fields are simply equated for the M-cones, and judged as different if a critical S-cone threshold is exceeded. A threshold ellipse is shown. Under Weber's Law this has the equation:

$$\frac{(\Delta \log M)^2}{(w_M)^2} + \frac{(\Delta \log S)^2}{(w_S)^2} = 1 \qquad \text{(A1)}$$

where w_S and w_M are the Weber fractions for S- and M-cones, respectively, S and M are the cone excitations [which can include added terms analogous to absolute threshold term I_o in Fig. 3(a)], and $\Delta \log S$ and $\Delta \log M$ are the differences in the natural logs of these cone excitations between the standard and matching fields.

The match point representing equality of test and reference fields is thus represented by the origin of coordinates at the center of the ellipse, where $\Delta \log S$ and $\Delta \log M$ are zero. Along the ascending diagonal through that match point (the line $\Delta\lambda = 0$ in Fig. 7), the equality of $\Delta \log S$ and $\Delta \log M$ implies that only the intensity of the match or reference field changes (match and reference field remain matched in wavelength). Other lines parallel to this each specify various intensities of some other matching field that differs more or less in color from the reference field. For small color differences, the wavelength difference $\Delta\lambda$ will be approximately proportional to the difference in $\log(S/M)$. The proportionality constant k is the derivative $d\lambda/d\log(S/M)$ (Fig. 2, bottom panel).

$$\begin{aligned} \Delta\lambda &= k\Delta\log\left(\frac{S}{M}\right) \\ &= k(\Delta \log S - \Delta \log M). \end{aligned} \qquad \text{(A2)}$$

Thus, in Fig. 7, the negative diagonal through the match point is a $\Delta\lambda$ axis.

For M-cone equated fields ($\Delta \log M = 0$), the threshold value of $\Delta \log S$ is w_S, the ellipse semiaxis in the $\Delta \log S$ (vertical) direction, and the value of $\Delta\lambda$ needed to achieve this is kw_S.

Note, however, that at a slightly lower intensity (represented by a movement down the line of slope 1 that characterizes the reference field's color) this reference field becomes indiscriminable, falling inside the threshold ellipse. To be discriminable at any intensity, a shorter wavelength reference field must lie on or above the line of slope 1 that is tangent to the threshold ellipse. From (A1) the slope of the threshold ellipse is $-\left(\frac{w_M}{w_S}\right)^2\left(\frac{\Delta \log M}{\Delta \log S}\right)$. Hence at the tangent point $\Delta \log M = -\Delta \log S\left(\frac{w_M}{w_S}\right)^2$. By substitution in (A1) this yields:

$$\left(\Delta \log M = -\frac{w_M^2}{\sqrt{w_M^2 + w_S^2}},\ \Delta \log S = \frac{w_S^2}{\sqrt{w_M^2 + w_S^2}}\right)$$

for the coordinates of the tangent point. The ellipse aspect ratio, w_S/w_M has a value of roughly 5 (Stiles, 1959), although the figure is drawn with a less extreme ratio for clarity. The more vertically elongated the threshold ellipse, the closer the tangent point comes to the top of the ellipse.

The Helmholtz prediction for the wavelength discrimination threshold vector is the value of $\Delta\lambda$ at the tangent point, rather than the value at the top of the ellipse, as in our simpler model. Applying (A2), the ratio of these wavelength difference thresholds evaluates to:

$$\sqrt{1 + \left(\frac{w_M}{w_S}\right)^2}.$$

For $w_S/w_M = 5$, the simplified color difference threshold computed for M-cone equated fields is only 2% less than the Helmholtz prediction, so the two predictions are practically equivalent at the level of accuracy involved here.

Our simple model can also be applied to discriminations made by other cone types. The worst case underestimation of threshold is incurred by assuming equality of the fields for one of two cone types

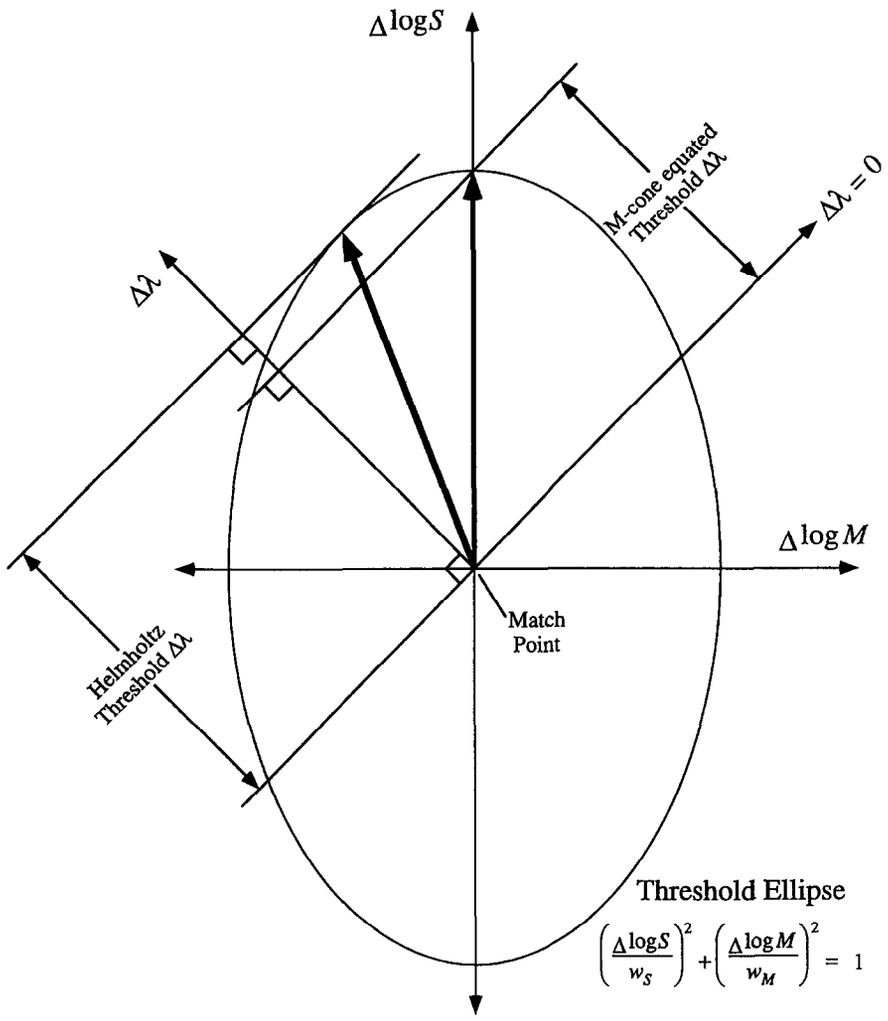

FIGURE 7. Threshold ellipse in log cone excitation space. Diagonal axes correspond to variations in log intensity and in wavelength.

that are equally sensitive. In this case the threshold is underestimated by a factor of 0.707, or 0.15 log units. Moreover, this underestimation factor is constant to the extent that the threshold ellipse aspect ratio is constant.

In our experiments, the discrimination measure is the standard deviation of matches, rather than a wavelength difference considered just noticeable by the subject, but analogous considerations apply. The standard deviation of log$S$ for M-cone equated stimuli (and the threshold $\Delta\lambda$ from our simplified model) are proportional to w_S, and the variances to w_S^2. In our experiment, however, adjustments in both wavelength and intensity were permitted in the search for a match, so $\Delta\lambda$ represents the algebraic sum of the mismatches in log$S$ and log$M$ [(A2)]. If log$M$ and log$S$ are uncorrelated in the chosen matches, the variance in log$M$ contributes to the variance in $\Delta\lambda$ a component proportional to w_M. The ratio of the standard deviation in $\Delta\lambda$ from two-dimensional matches to the standard deviation along the M equality line is:

$$\sqrt{1 + \left(\frac{w_M}{w_S}\right)^2}$$

as before, again a negligible difference if w_S/w_M is large.